NEOPLASIA
www.neoplasia.com

Volume 17 Number 8 August 2015 pp. 613–624 613

Pleiotrophin Exerts Its Migration and Invasion Effect through the Neuropilin-1 Pathway

Rania Elahouel[*], Charly Blanc[†], Gilles Carpentier[*], Sophie Frechault[*], Ilaria Cascone[*], Damien Destouches[*], Jean Delbé[*], José Courty[*] and Yamina Hamma-Kourbali[*]

*Laboratoire de Recherche sur la Croissance Cellulaire, la Réparation et la Régénération Tissulaires (CRRET), CNRS; Université Paris-Est Créteil, France; †INSERM, U955, Equipe 7, 94000 Créteil, France; Université Paris-Est, Faculté de médecine, 94000 Créteil, France

Abstract

Pleiotrophin (PTN) is a pleiotropic growth factor that exhibits angiogenic properties and is involved in tumor growth and metastasis. Although it has been shown that PTN is expressed in tumor cells, few studies have investigated its receptors and their involvement in cell migration and invasion. Neuropilin-1 (NRP-1) is a receptor for multiple growth factors that mediates cell motility and plays an important role in angiogenesis and tumor progression. Here we provide evidence for the first time that NRP-1 is crucial for biological activities of PTN. We found that PTN interacted directly with NRP-1 through its thrombospondin type-I repeat domains. Importantly, binding of PTN to NRP-1 stimulated the internalization and recycling of NRP-1 at the cell surface. Invalidation of NRP-1 by RNA interference in human carcinoma cells inhibited PTN-induced intracellular signaling of the serine-threonine kinase, mitogen-activated protein MAP kinase, and focal adhesion kinase pathways. Accordingly, NRP-1 silencing or blocking by antibody inhibited PTN-induced human umbilical vein endothelial cell migration and tumor cell invasion. These results suggest that NRP-1/PTN interaction provides a novel mechanism for controlling the response of endothelial and tumoral cells to PTN and may explain, at least in part, how PTN contributes to tumor angiogenesis and cancer progression.

Neoplasia (2015) 17, 613–624

Introduction

The heparin-binding growth factor pleiotrophin (PTN), also known as *heparin affin regulatory peptide*, is a secreted 18-kDa protein, which, along with midkine, constitutes a two-member family of regulatory peptides. During embryonic development, PTN is mainly expressed in neuroectodermal and mesodermal tissues, indicating its role in neuron migration and epithelium-mesenchyme interactions [1,2]. PTN expression is limited in adults, except at such sites as mammary gland and uterus, which are associated with reproductive angiogenesis [3,4]. Studies of the pathological involvement of PTN indicate that this molecule may be considered a proto-oncogene [3,5] over-expressed in various malignant human tumors and tumor cell lines, such as breast, prostate, colon, and skin, as well as being involved in tumor angiogenesis and metastasis [2,6–8].

PTN consists of two random coiled clusters of basic residues (N- and C-terminal) and two β-sheet domains. Each β-sheet domain contains a thrombospondin repeat I (TSR-I) motif, which has been suggested to be responsible for the interaction of PTN with heparin [9]. Previous studies have demonstrated that both the TSR domain and the C-terminal regions of PTN are particularly implicated in its biological activities [9,10]. These biological activities of PTN are mediated by four distinct receptors: SDC3 (N-syndecan) [11], protein tyrosine phosphatase (RPTP β/ζ) receptor [12], anaplastic lymphoma kinase (ALK) [13], and cell-surface nucleolin [14].

Address all correspondence to: Yamina Hamma-Kourbali, INSERM, U955, Equipe 7, 8 rue du général Sarrail, 94000 Créteil, France; Université Paris-Est, Faculté de médecine, 94000 Créteil, France.
E-mail: Yamina.HAMMA@inserm.fr
Received 6 March 2015; Revised 16 July 2015; Accepted 29 July 2015

1476-5586
http://dx.doi.org/10.1016/j.neo.2015.07.007

N-syndecan and RPTP β/ζ have been implicated in neurite outgrowth [11], whereas cell-surface nucleolin, RPTP β/ζ, and ALK have been shown to mediate PTN-induced mitogenic, migratory, angiogenic, and transforming activities [6,13,15] in a process mediated by the phosphatidylinositol 3-kinase and MAP kinase signaling pathways [13]. Apart from its growth stimulatory activities described above, PTN was also shown to inhibit angiogenesis through interaction with vascular endothelial growth factor A165 (VEGF A_{165}) [16].

Neuropilin-1 (NRP-1), a type I transmembrane protein, was originally identified as co-receptor for class-3 semaphorins implicated in axonal chemorepulsive guidance in the developing nervous system [17] and for VEGF A_{165} during vascular development [18]. *NRP-1*–null mice display a lethal embryonic phenotype characterized by dramatic vascular and cardiac defects [19] and overexpression of NRP-1 in mouse embryos, which result in ectopic sprouting and nerve fiber defasciculation with excess capillary growth and malformed hearts [20]. NRP-1 and the closely related protein NRP-2 share 44% amino-acid sequence identity and a common structure comprising a large extracellular region that contains two complement binding-like CUB domains, two coagulation factor FV/FVIII homology domains, a meprin MAM domain, and a transmembrane domain with a short cytoplasmic region [21]. The two complementary binding-like CUB domains and the FV/FVIII homology domains are involved in binding of semaphorin 3A, whereas the VEGF binding domain involved only the FV/FVIII homology domain. The cytoplasmic domain of NRP-1 consists of 44 amino acids and contains a C-terminal three–amino-acid PDZ-domain motif, SEA, which binds to the PDZ domain protein, GIPC (GAIP-interacting protein C-terminus) [21].

NRP-1 is well known to be implicated in tumor angiogenesis and cancer progression [22]. It has been found to be upregulated in various cancers and correlates with tumor growth, disease progression, and poor patient prognosis [23,24]. In several kinds of cancer, targeting NRP-1 has been found to decrease tumor growth and associated angiogenesis [25,26]. In support of the involvement of NRP-1 in several proliferative diseases, it has been shown that NRP-1 binds several heparin-binding molecules, such as fibroblast growth factor family (FGF) [22], platelet-derived growth factor [22], and hepatocyte growth factor (HGF) [22]. Additional data have indicated that NRP-1 potentiates the biological activity of these growth factors, showing that the involvement of NRP-1 in proliferative and angiogenic activities is not restricted to VEGF [22,27]. Based on these observations, the aim of the present study was to determine whether NRP-1 binds to PTN and to investigate the biological consequences of such possible interaction.

Materials and Methods

PTN Constructs and Antibodies

Human recombinant PTN (rPTN) of bacterial origin was produced and purified as previously described [3]. Human FGF2 and VEGF A_{165} growth factors were from Sigma. $PTN_{1\text{-}136}$ and mutated PTN ($PTN_{9\text{-}59}$, $PTN_{60\text{-}110}$, and $PTN_{9\text{-}110}$) coupled to glutathione *S*-transferase (GST) were produced in bacteria and purified in the laboratory by sequential heparin-Sepharose and Mono-S chromatography, as previously described [16]. Recombinant human NRP-1 chimera fused via its carboxy-terminal region to a polyhistidine-tag (rNRP-1) was purchased from R&D Systems.

Rabbit monoclonal anti-human NRP-1(MABD62C6), rabbit polyclonal anti-p44/42 MAPK (#9102), anti-Akt (#9272), anti-phosphorylated p44/42 MAPK (thr202/tyr204, #4370), anti-phosphorylated Akt (Ser473, #9271), and anti-phosphorylated FAK (Tyr 925, #3284) were purchased from Cell Signaling Technology. Rat monoclonal anti-human RPTPβ/ζ (MAB2688), sheep anti-human NRP-1 (CD304), and goat polyclonal anti-human pleiotrophin (AF-252-PB) were obtained from R&D Systems. Rabbit polyclonal anti-human ALK (aa 426-528) was from Zymed. Anti-GAPDH (clone 6C5) was obtained from Ambion. Secondary antibodies were purchased from Jackson Immunoresearch.

Cell Culture

Primary human umbilical vein endothelial cells (HUVECs, Promocell) were cultured with the EGM-2 Bullekit supplied by Clonetics (Lonza) until passage 3. Human prostate carcinoma PC3 cells and mammalian carcinoma MDA-MB231 cells were provided by the American Type Culture Collection and grown respectively in RPMI or Dulbecco's modified Eagle's medium supplemented with 5% FBS. All cells were cultivated at 37°C under a 5% CO_2 humidified atmosphere.

Western Blotting

Samples were separated by SDS-PAGE under reducing conditions and then transferred onto 0.45-μm Immobilon-P membrane (Millipore) using standard protocols. Nonspecific binding was prevented by incubating the membrane for 1 hour at room temperature (RT) in 5% (w/v) BSA in PBS containing 0.2% (v/v) Tween-20 (blocking buffer; BB). Membranes were subsequently incubated overnight at 4°C with primary antibodies against NRP-1, phosphorylated or unphosphorylated ERK, Akt, and FAK (Cell Signaling) at 1 μg/ml in BB and then with rabbit secondary antibodies at 80 ng/ml BB for 1 hour at RT. Immunocomplexes were visualized using a chemiluminescence detection system kit (Roche Diagnostics).

For phosphorylation assays, PC3 cells (4×10^5) were seeded onto six-well plates in RPMI supplemented with 5% FBS and grown to subconfluency. Cells were then incubated overnight in serum-free medium before addition of PTN (50 ng/ml) for 5 and 15 minutes. Cells were washed twice with warm PBS and lysed with 50 μl of hot Laemmli buffer 2 × (95°C). Samples (10 μg) were analyzed by Western blotting.

For immunoprecipitation, cells were treated as above and then lysed in buffer containing 10 mM Tris-HCl pH 7.5, 100 mM NaCl, 4% NP40, 50 mM EDTA, and protease inhibitors (1 μg/ml leupeptin, pepstatin, and aprotinin, and 1 mM phenylmethylsulfonyl fluoride) (Sigma Aldrich). Equivalent quantities of proteins (1 mg) were incubated with or without 100 ng/ml of PTN overnight at 4°C. PTN was then immunoprecipitated with 1 μg of anti-PTN antibody overnight, followed by 3 hours of incubation with G-Sepharose beads (GE Healthcare). Beads were then washed with lysis buffer, and the recovered proteins were analyzed by SDS-PAGE.

In pull-down experiments, cell lysates were prepared as described above. Samples (1 mg) were first precleared with GST beads (Amersham) for 1 hour at 4°C to avoid nonspecific interactions. Samples were then incubated overnight at 4°C with equivalent amounts (2 μg) of GST fusion proteins, including $PTN_{1\text{-}136}$, $PTN_{9\text{-}59}$, $PTN_{60\text{-}110}$, and $PTN_{9\text{-}110}$. For competition experiments, PC3 cell lysate was incubated with GST- $PTN_{1\text{-}136}$ with or without a 10-fold excess of VEGF A_{165} or bFGF. After overnight incubation, samples were incubated with glutathione-Sepharose beads for 3 hours. Beads were then washed with

lysis buffer and resuspended in 2× concentrated electrophoresis sample buffer (125 mM Tris-HCl pH 6.8, 4% SDS, 10% glycerol, 0.6% bromophenol blue, 5% β-mercaptoethanol), and the recovered proteins were analyzed by SDS-PAGE.

Binding Assays

Cell binding assay was carried out according to the protocol provided in Bermek et al. [7]. Cells (10^5) were plated onto 96-well plates overnight and then serum-starved for 24 hours. Cells were then incubated for 2 hours at 4°C with rPTN in the presence or absence of rNRP-1, as indicated. After three washings in PBS/0.2% Tween 20 (v/v), bound PTN was detected. Anti-human PTN antibody (R&D) at 250 ng/ml in PBS/BSA 1% (w/v) and revealed by HRP-conjugated anti-goat IgG antibody (Jackson Immunoresearch). Peroxidase activity was detected using the TMB Substrate Kit (Pierce), stopped by addition of 1 M H_2SO_4, and measured by spectrophotometry at 450 nm.

For ELISA-based binding assays, rNRP-1 (4 μg/ml) diluted in PBS was coated overnight at 4°C on 96-well ELISA plates. The wells were washed twice with PBS containing 0.05% Tween 20 and saturated with PBS containing 3% BSA for 1 hour at RT. rPTN was then added to the wells and incubated overnight at 4°C. Plates were washed three times with PBS/Tween 0.5%, and bound PTN was detected as described above in cell-binding assays.

Biochemical Quantification of NRP-1 Cell Surface

Purification of biotinylated surface membrane proteins cells was achieved using the Pierce Cell Surface Protein Isolation Kit according to the manufacturer's instructions. Biotinylated protein concentrations were determined using BCA protein assay. Biotinylated NRP-1 levels were analyzed by Western blot as described above.

siRNA Transfection

For siRNA transfection, experimental conditions were optimized, especially for HUVECs. siRNA experiments were carried out in serum- and antibiotic-free Opti-MEM medium (GIBCO) using RNAi MAX transfect agent (Invitrogen). Cells were plated overnight at 50% to 70% confluence and then transfected with 10 nM of either nontargeting siRNA as a control or target-specific siRNAs to knock down NRP-1 (FlexiTube siRNA # SI02663213, QIAGEN). Transfection efficiency was evaluated by Western blot analysis. Cells were used lysed or tested in functional assays 24 to 72 hours after transfection.

Immunofluorescence Microscopy

PC3 cells were plated on glass slides and serum-starved overnight, before incubation at 37°C with 100 ng/ml of PTN for indicated times. Cells were fixed for 10 minutes with 4% paraformaldehyde, washed in PBS, permeabilized with 0.1% Triton X-100, and then saturated for 20 minutes with 3% (w/v) BSA. Cells were incubated with anti-human NRP-1 diluted 1/200 in PBS/BSA 1% at 4°C overnight. Cells were washed 3 × 5 minutes with PBS and incubated at room temperature for 1 hour with FluoProbes 547H donkey anti-sheep IgG (Interchim) diluted 1/200 in PBS/BSA 1% containing DAPI 1 μg/ml. After 3 × 5-minute washes, cells were mounted with MOWIOL (Calbiochem).

Confocal fluorescence images were acquired using an IX81 inverted Olympus microscope equipped with a DSU spinning disk confocal system (Olympus France) coupled to an Orca R2 CCD camera (Hamamatsu Corporation, Japan). Observations were made using the 60× objective (oil immersion NA 1.25). Cells were analyzed by acquiring axial *z* stacks of confocal images (8 μm from the base to the top in 0.5-μm steps). Image processing was done using ImageJ software [28]. Residual blurring was removed by spatial deconvolution: Point-Spread Function (PSF) was calculated using the ImageJ plugin PSF Generator [29], and deconvolution properly speaking was carried out using the Richardson-Lucy algorithm used with the Deconvolution Lab ImageJ plugin [30]. The latter two freeware are available from the EPFL (Ecole Polytechnique Fédérale de Lausanne [Biomedical Imaging Group]), Lausanne. Switzerland. « Fire » look-up table was used in merged representations to improve visibility of the NRP-1 labeling, without altering linearity of the signal.

Migration and Invasion Assays

Migration assays were accomplished using a 24-well chemotaxis chamber (Transwell, BD Biosciences). Pore size 8-μm polycarbonate filters were coated with 10 mg/ml of type I collagen (Serva). A total of 1×10^5 cells in EBM-2 medium supplemented with 1% FBS were plated into the upper chamber of Transwell chamber in the presence of PTN alone or with PTN and an anti–NRP-1 blocking antibody, or IgGs control (R&D System) were added to the lower chamber. Cells were allowed to migrate for 6 hours at 37°C. Nonmigrated cells were then removed by wiping with a cotton tip, and migrated cells were fixed with absolute ethanol and stained with crystal violet 0.2% (v/v) in ethanol 2%. Migrated cells in three fields of each well (Leitz Aristoplan microscope, ×10 objective) were quantified by image analysis. Briefly, a parameterized extraction of the blue color was followed by a threshold ("Otsu" method [31]) and a subsegmentation (watershed method [32]) to determine the number of cells.

In invasion assay, PC3 cells (2×10^4) were suspended in serum-free medium and seeded onto Matrigel (BD Biosciences)-coated Transwell chamber (20 μg/well). Medium with or without PTN supplemented with anti–NRP-1 IgG or nonimmune IgG (R&D system) was introduced into the lower chamber. Invasion was carried out for 14 hours at 37°C. Cells were fixed and treated, and the number of invading cells was determined as described above for migration assay.

Statistical Analysis

Values are reported as means ± SEM. Statistical significance was determined by the analysis of variance unpaired *t* test using GraphPad Prism 4.0 software. Values of $P < .05$ were considered significant.

Results

NRP-1 and PTN Growth Factor

To determine whether PTN interacts with NRP-1, we first checked NRP-1 expression levels in four cell cultures, including those that express NRP-1, such as PC3 and MDA-MB231, HUVEC, as well as in Chinese hamster ovary (CHO) cells, which do not express NRP-1. The NRP-1 expression level was evaluated using Western blot analysis and showed that, as expected, both tumor and endothelial cells express high levels of NRP-1 [18], whereas no expression was detected in CHO cell lines (Figure 1*A*).

An immunoprecipitation experiment using anti-PTN antibody was used to investigate the interaction of PTN with NRP-1 in these sets of cells. In PC3, MDA-MB231, and HUVEC cells, 130-kDa mature NRP-1 co-immunoprecipated with PTN (Figure 1*B*). No immunoreactivity was revealed with extracts from CHO cells (data

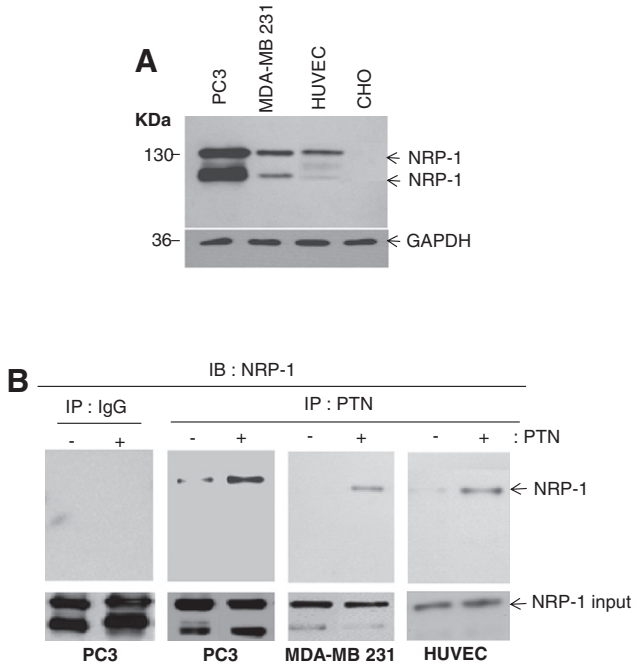

Figure 1. Identification of NRP-1 as PTN-binding protein. (A) NRP-1 expression in different cell lines including human prostate cancer cells (PC3), human breast adenocarcinomas (MDA-MB231), HUVEC, and CHO cells. Cell lysates were separated by SDS-PAGE and immunoblotted with anti–NRP-1 antibodies and anti-GAPDH antibodies (loading control). (B) PTN interacted with NRP-1. Cell lysates were incubated with (+) or without (−) 100 ng/ml of PTN overnight at 4°C. PTN was then immunoprecipitated (IP) with anti-PTN antibodies or with nonimmune IgG. Immunoprecipitates were immunoblotted (IB) with anti–NRP-1 antibody. Immunoblot with anti–NRP-1 of input lysate for each cell line is shown in the bottom panel of IP. The apparent molecular mass of markers is indicated in kDa; and the migration of the NRP-1 protein, by the arrow on the right.

not shown) or with control IgG (Figure 1*B*). These results indicate that PTN directly or indirectly interacted with NRP-1.

PTN TSR-I Domains and NRP-1 Binding

We next asked whether the two PTN TSR-I domains were involved in its interaction with NRP-1. To answer this question, pull-down experiments using various GST-PTN fusion proteins on PC3 lysates were carried out. As expected, whole GST-PTN$_{1\text{-}136}$ fusion protein formed a complex with NRP-1 (Figure 2*A*), confirming the results observed in Figure 1. In contrast and as a control, either in the absence of GST-PTN$_{1\text{-}136}$ or of GST alone or with BSA, no signal was observed. However, GST-PTN$_{1\text{-}136}$ fusion protein was able to pull down ALK and RPTPβ/ζ, known PTN receptors (data not shown). Then, we carried out pull-down experiments of the N- and C-TSR-I domains using corresponding GST-PTN$_{9\text{-}59}$, GST-PTN$_{60\text{-}110}$, and GST-PTN$_{9\text{-}110}$ fusion proteins (Figure 2*B*). The GST-PTN$_{9\text{-}59}$ fusion protein did not pull down NRP-1, in contrast with the GST-PTN$_{60\text{-}110}$, which displayed NRP-1 binding corresponding to 45% of that observed for GST-PTN$_{1\text{-}136}$. GST-PTN$_{9\text{-}110}$ fusion protein corresponding to a full TSR-I domain pulled down NRP-1 to an extent similar to that observed for GST-PTN$_{1\text{-}136}$. Altogether, these results suggest that the C-TSR-1 domain is involved in PTN/NRP-1 interaction, but this interaction is more effective in the presence of the full N- and C- TSR-1 domains, corresponding to 9 to 110 amino acids (Figure 2*B*).

Because NRP-1 binds multiple mitogenic and angiogenic growth factors, such as vascular endothelial growth factor (VEGF A$_{165}$) and basic fibroblast growth factor (bFGF, FGF2), we carried out a pull-down experiment with GST-PTN$_{1\text{-}136}$ in the presence of VEGF A$_{165}$ or FGF2. As shown in Figure 2*C*, a 10-fold molar excess of VEGF A$_{165}$ or FGF2 significantly inhibited the binding of GST-PTN$_{1\text{-}136}$ to NRP-1, suggesting that PTN, FGF2, and VEGF A$_{165}$ display overlapping NRP-1 domain interaction.

PTN Binding to NRP-1

To investigate whether PTN binds directly or indirectly to the NRP-1 receptor, binding experiments were carried out using rNRP-1. PTN was found to bind in a dose-dependent manner to cells whose saturation value reached 5 μg/ml for PC3 and HUVECs and 2 μg/ml for MDA-MB231 cells (Figure 3*A*). Based on these results, we examined whether rNRP-1 interfered with PTN binding to the cell surface. As shown in Figure 3*B*, rNRP-1 inhibited the binding of PTN in a dose-dependent manner. Maximal binding inhibition was observed at 0.5 μg/ml rNRP-1. This inhibition remained constant even at higher concentration of rNRP-1, attaining inhibition rates of 45%, 50%, and 55% for PC3, MDA-MB231, and HUVEC cells, respectively. These results suggest that PTN binds to cells via NRP-1 and probably via other PTN receptors, such as ALK and RPTP β/ζ. In addition, as heparin binding growth factors, PTN binds to the high-affinity binding sites ALK and RPTPβ/ζ receptors [33] and to the low-affinity binding sites; theses last sites are mainly sulfated glycosaminoglycans [34]. These low-affinity binding sites can be, according to the cell types, 10^5- to 10^6-fold more numerous than the number of the high-affinity binding sites.

To further study whether PTN interacts directly with NRP-1, we used an ELISA-based assay in which rNRP-1 was immobilized. PTN bound specifically and in a dose-dependent manner to immobilized rNRP-1, whereas a BSA control bound very weakly to rNRP-1, corresponding to nonspecific binding (Figure 3*C*). These results indicate that PTN could bind directly to the NRP-1 receptor.

Effects on Cell Surface NRP-1 and Its Internalization

PTN treatment induced a decrease in NRP-1 at the cell surface (Figure 4*A*). After 15 and 30 minutes of treatment, this diminution was respectively around 40% and 47%. Surprisingly, 2 hours after PTN cell stimulation, the NRP-1 cell surface level increased to 72% of that found with unstimulated cells. VEGF A$_{165}$ used as a positive control reduced cell surface NRP-1 by 55% after 30 minutes of stimulation, confirming the results described by Narazaki et al. [35]. These results suggest that following stimulation, PTN cell surface NRP-1 is internalized and then after recycled partially to the plasma membrane. Furthermore, quantification of the total NRP-1 level revealed the same distribution profile as cell surface NRP-1, namely, reduction at 15 and 30 minutes followed by an increase after 2 hours (Figure 4*A*).

To better understand NRP-1 cell trafficking, confocal analysis was further carried out in PC3 cells treated or not with PTN (Figure 4*B*). In unstimulated cells, NRP-1 was detectable more intensely at the cell surface, whereas after 15 and 30 minutes of stimulation, NRP-1 was more intensely observed in the cytoplasm and in the perinuclear region, with dot-like distribution, corresponding to localization in internalized vesicles. After 1 hour of stimulation, NRP-1 vesicles were mainly redistributed to the cell surface (Figure 4*B*), in agreement with biochemical analysis. All

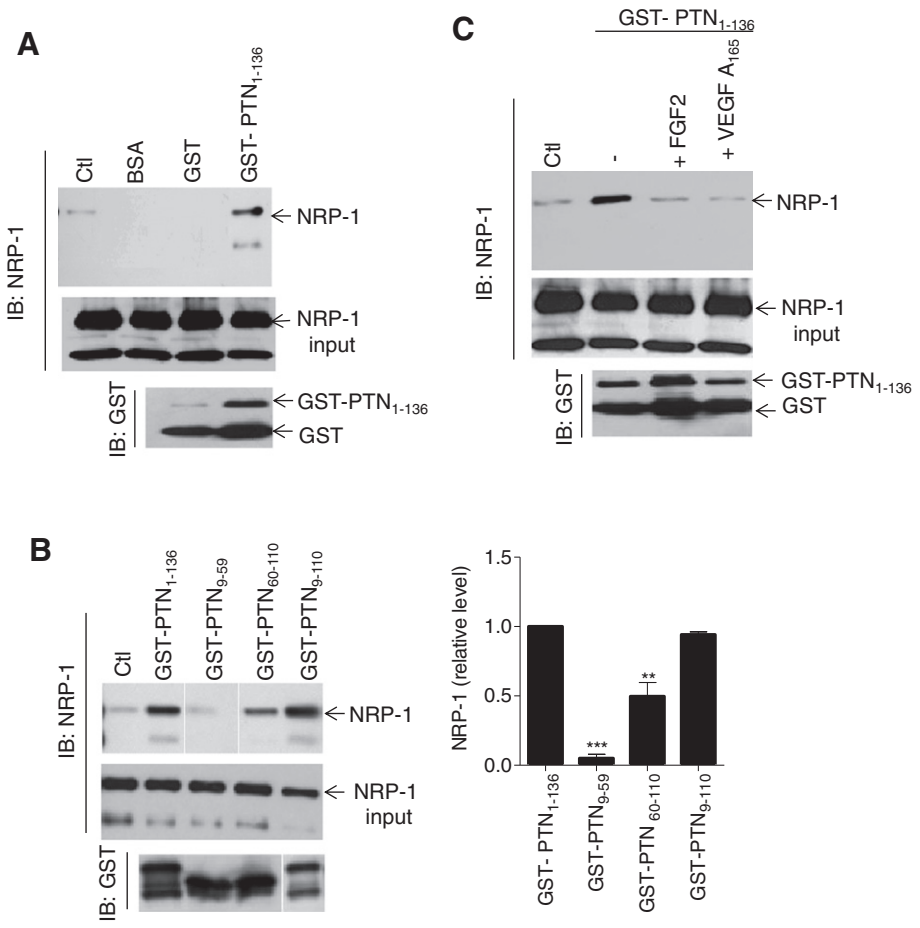

Figure 2. NRP-1 interaction with GST-PTN fusion protein. (A) Binding of PTN-GST to NRP-1. PC3 cell lysate was incubated with PTN-GST (2 μg), without (control), with GST protein alone, or with BSA followed by incubation with glutathione-Sepharose beads. The presence of NRP-1 was determined by IB using anti–NRP-1 antibodies. As control, the input lysates were blotted with anti–NRP-1 and anti-GST antibodies, respectively, as indicated at the bottom of IP. (B) The two TSR-1 homology motifs of the β-sheet domains of PTN are required for PTN–NRP-1 interaction. The fusion proteins GST-PTN_{1-136}, GST-PTN_{9-59}, GST-PTN_{60-110}, and GST-PTN_{9-110} were incubated with PC3 lysate followed by incubation with glutathione-Sepharose beads. Immunoblotting was done as described above. The NRP-1 protein content was determined by densitometry analysis and normalized to control. Results shown are representative of three independent experiments. Bars, SEM. $^{**}P < .01$; $^{***}P < .001$ versus control. (C) The heparin binding growth factors FGF-2 or VEGF A_{165} compete with PTN for binding to NRP-1. PC3 cell lysate was incubated with PTN-GST alone (−) or in the presence of 10-fold excess of indicated growth factors followed by incubation with glutathione-Sepharose beads. Immunoblotting was done as described above.

these results suggest that NRP-1 is internalized after PTN treatment and partially recycled within 2 hours to the cell surface.

Induction of Signal Transduction through NRP-1

Previous studies in our and others' laboratories have shown that PTN activates the serine-threonine kinase Akt, mitogen-activated protein MAP kinase (MAPK p44/42), and focal adhesion kinase (FAK) pathways [3,13,36]. Treatment of PC3 cells with PTN produced an increase in the phosphorylation of MAPK, Akt, and FAK (tyr 925) after 15 minutes (Figure 5*B*). Transfection of cells with NRP-1 siRNA resulted in successful inhibition of NRP-1 expression in comparison with control nontargeting siRNA (Figure 5*A*). Accordingly, NRP-1 silencing in PC3 cells prevented phosphorylation of MAPK induced by PTN, whereas it was not affected by siRNA control transfection. Similarly, in the NRP-1 silencing cells, PTN-stimulated Akt and FAK_{925} phosphorylation was markedly attenuated (respectively, around 60% and 80% inhibition) compared with the stimulated control (Figure 5*B*). These results demonstrate that NRP-1 could act as a receptor or co-receptor that participates in PTN-induced cell signaling.

Next, we investigate the relevance of NRP-1 on MAPK, Akt, and FAK_{925} phosphorylation pathways in PC3 cells treated with heparin growth factors FGF2 and VEGF A_{165} that interfere with the PTN/NRP-1 interaction as described above. As expected, VEGF A_{165} and FGF2 induced MAPK, Akt, and FAK_{925} phosphorylation (Figure 5, *C–D*). NRP-1 knockdown had no effect on VEGF A_{165}–induced phosphorylation of MAPK and FAK_{925} and had a weak effect on the Akt phosphorylation (around 30%) (Figure 5*C*). FGF2-induced phosphorylation of Akt and FAK_{925} was also not inhibited by NRP-1 siRNA; however, phosphorylation of MAPK p44/42 was reduced by 40% (Figure 5*D*). These results indicated a specific signaling pathway for PTN/NRP-1 interaction in the regulation of cell motility.

Tumor Cell Invasiveness and EndothelialCell Migration

Having established that NRP-1 played a prominent role in regulating PTN-induced cell signaling, we investigated the biological

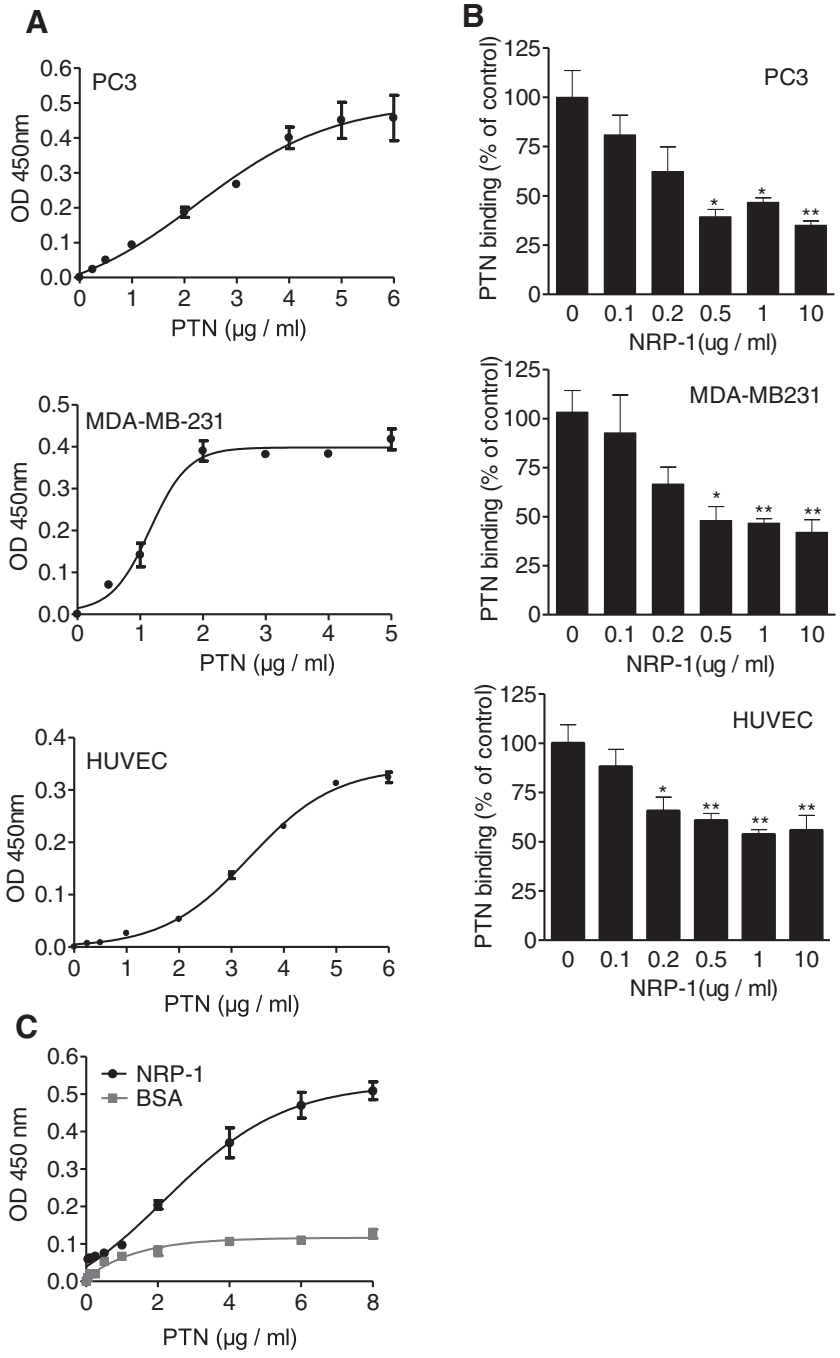

Figure 3. rNRP-1 specifically inhibits PTN binding to cells. (A) PTN binding to PC3, MDA-MB231, and HUVEC cells. Cells were incubated at 4°C for 2 hours with increasing concentrations of PTN ranging from 0 to 6 μg/ml. (B) Cells were incubated at 4°C for 2 hours with 2 μg/ml PTN and increasing concentrations of rNRP-1 ranging from 0 to 5 μg/ml. Bars, SEM. *$P < .05$; **$P < .01$ versus control. (C) PTN bound directly to NRP-1. Microtiter plates were coated with rNRP-1 or BSA and incubated with increasing concentrations of PTN (0 to 8 μg/ml). Bound PTN was detected by ELISA-based measurement of streptavidin-HRP staining. The results represent the means of three experiments.

effects of NRP-1/PTN interaction. Firstly, NRP-1 expression was silenced in PC3 cells by siRNA NRP-1, and its effect on PTN-induced PC3 invasion through the Matrigel layer was examined. In the absence of PTN, control and NRP-1 siRNA silencing resulted in comparable basal levels of PC3 cell invasion (Figure 6*A*). In the presence of PTN, PC3 cell invasion was stimulated 1.8-fold compared with the unstimulated control. Whereas stimulation of PC3 cell invasion induced by PTN was not affected by transfection of the siRNA control, NRP-1 silencing inhibited PTN-induced PC3 cell invasion to the basal level (Figure 6*A*). Secondly, to confirm the role of NRP-1 in cell invasion, we analyzed the effect of the anti–NRP-1 blocking antibody on PTN-induced invasion of PC3 cells. Accordingly, the anti–NRP-1 antibody inhibited PTN-induced PC3 cell invasion in a dose-dependent manner, and total inhibition was achieved at 5 µg/ml (Figure 6*B*). The nonimmune IgG control had no effect on PTN-induced PC3 cell invasion (data not shown).

We next evaluated NRP-1 involvement in PTN-mediated migration of endothelial cells. As shown in Figure 6*C*, without

PTN, the silencing of NRP-1 expression did not alter HUVEC migration. However, the stimulatory effect of PTN on HUVEC migration was completely abolished in NRP-1 silencing cells (Figure 6*C*). Moreover, NRP-1 blocking by NRP-1 antibody inhibited enhanced PTN-induced HUVEC migration in a dose-dependent manner and was completely inhibited at 5 μg/ml of NRP-1 antibody (Figure 6*D*). These data show that PTN-mediated migration required the presence of NRP-1.

Taken together, these results indicate that NRP-1 is necessary for PTN-induced cell migration and invasion.

Discussion

NRP-1 is expressed in a wide variety of human tumor cell lines and tumor patient biopsies, including those derived from carcinomas of the prostate, kidney, bladder, stomach, colon, pancreas, breast, ovary, and lung [22]. Increased expression of NRP-1 correlates with tumor aggressiveness and poor prognosis [24,37]. Preclinical data indicate that blockade of NRP-1 not only suppresses tumor growth and reduces tumor angiogenesis but also normalizes the remaining vasculature which counteracted tumor hypoxia and subsequent tumor invasiveness [26,38]. In addition to VEGF and semaphorin, other ligands, such as heparin-binding growth factors HGF, platelet-derived growth factor, and FGF-2, can bind to NRP-1 [22]. Like NRP-1, PTN is involved in nervous and cardiovascular system development, tumor growth, and angiogenesis, suggesting a possible interaction between these two molecules. The results we report here support the contention that PTN is a new NRP-1 ligand. On the other hand, NRP-1 is a new PTN receptor that mediates PTN-induced cell migration and invasion.

Using immunoprecipitation and pull-down experiments, we showed that PTN interacts with NRP-1 in PC3 and MDA-MB231 carcinoma and HUVEC cells. This interaction was direct, as demonstrated by immobilized soluble NRP-1 ELISA assays. Moreover, pull-down experiments demonstrated that PTN/NRP-1 interaction was disrupted in the presence of FGF-2 and VEGF A_{165} growth factors. This is consistent with the proposed role for NRP-1 as a common co-receptor that binds multiple ligands, such as FGF-2, HGF, and VEGF A_{165}[22]. These growth factors competed with PTN for binding to NRP-1, indicating that the binding domains for these growth factors on NRP-1 probably overlap. On the other hand, PTN binding to carcinoma and endothelial cells was blocked by soluble recombinant NRP-1. These results prompted us to investigate which molecular domain of PTN was involved in the binding to NRP-1. Our results indicate that $PTN_{60\text{-}110}$, which corresponds to

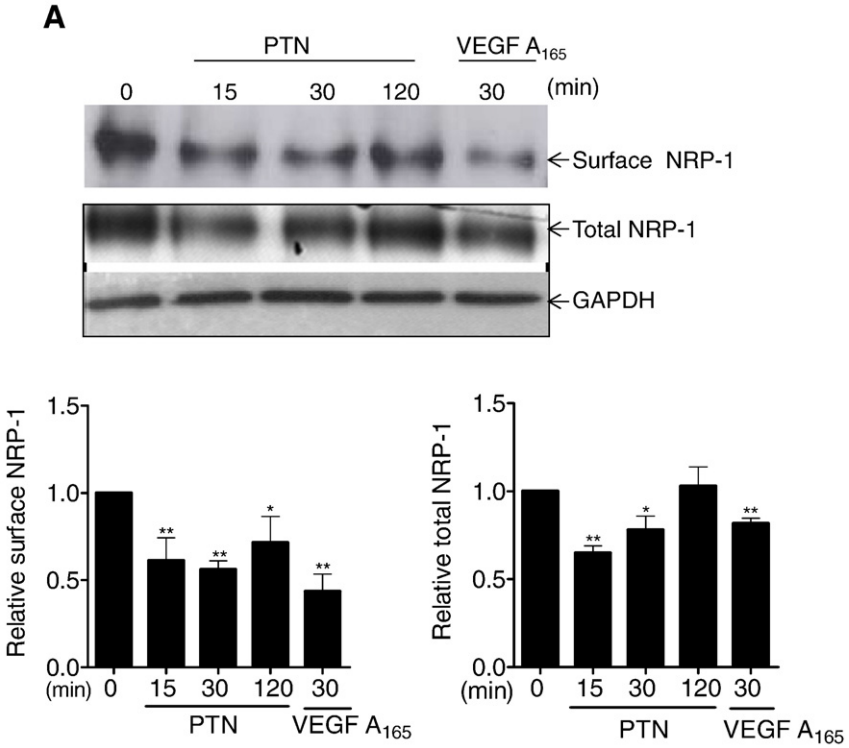

Figure 4. PTN reduces levels of cell surface NRP-1 and induces its internalization. (A) Analysis of cell surface NRP-1 in PTN-stimulated PC3 cells. PC3 cells were stimulated with PTN (100 ng/ml) for the indicated times. Cell surface proteins biotinylated as described in "Materials and Methods" were collected using streptavidin-agarose. Samples of total cell lysates or surface fraction were then analyzed by Western blotting with an anti–NRP-1 antibody. The total and cell surface NRP-1 contents were quantified by densitometry analysis (bottom graphs). Results shown are representative of three independent experiments. Bars, SEM. **P* < .05; ***P* < .01 versus control. (B) PTN induced the internalization of NRP-1. Serum-starved PC3 cells were incubated at 37°C for 0, 15, 30, or 60 minutes with PTN (100 ng/ml) or with VEGF A_{165} (100 ng/ml) for 30 minutes. Cells were then fixed and stained with anti–NRP-1 antibody and DAPI. Cell nuclei were visualized in middle panels, NRP-1 staining in middle and merged in bottom panels (NRP-1 ["Fire" look-up table] and nuclei [cyan]). "Fire" look-up table was used in the merged panels to improve visibility without altering linearity of the signal and to keep the same dynamic signal as the one present in the single-channel panels. This progressive pseudocolor palette (from black, purple, red, yellow, to white) permits a higher range of level of visualization of signal. Arrowheads indicate NRP-1. Scale bar, 10 μm.

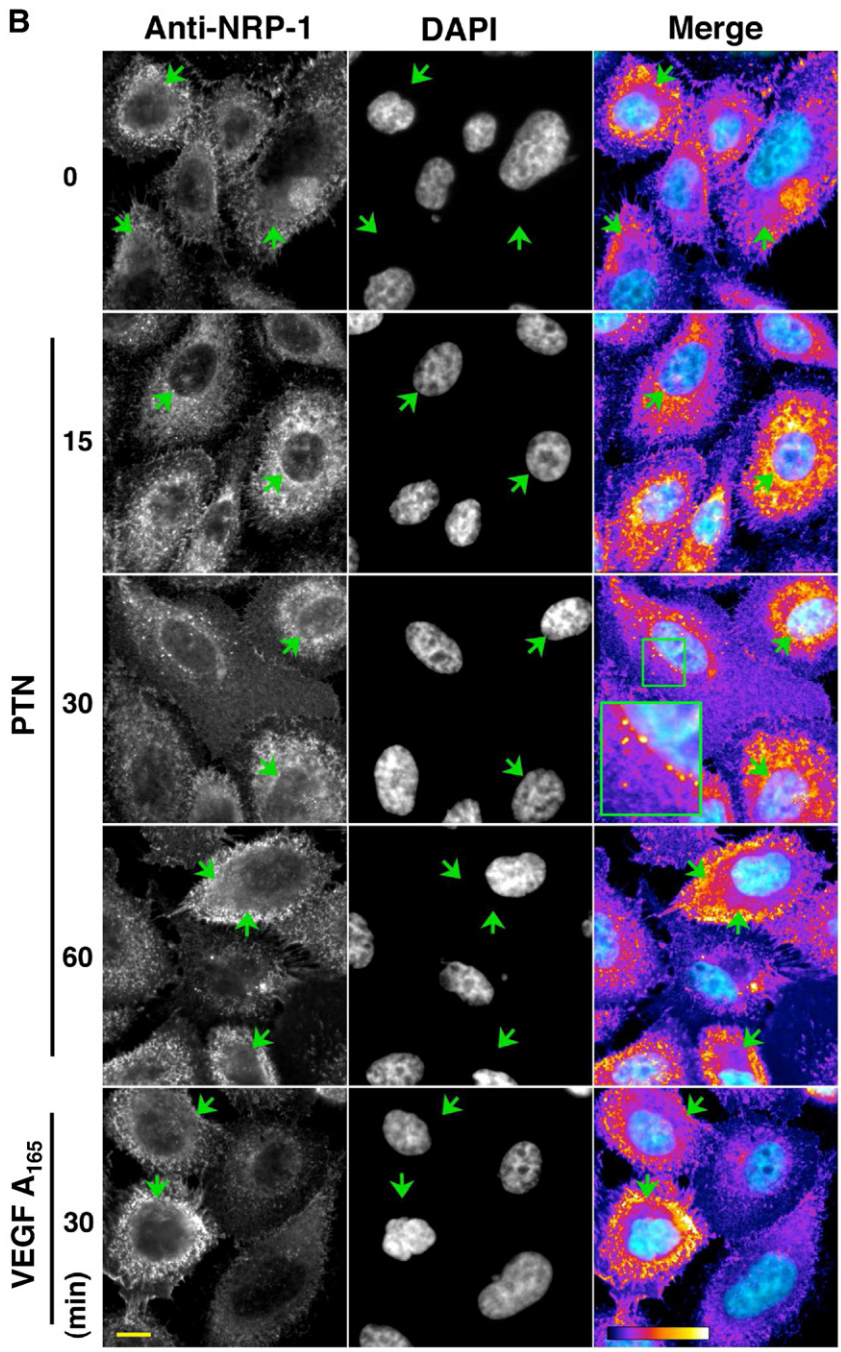

Figure 4. (*continued.*)

the C-TSR-I domain, was involved in the binding of PTN to NRP-1, but this was enhanced in the presence of the whole TSR-1 domains. Indeed, PTN contains two random coiled clusters of basic residues (N- and C-terminal) and two β-sheet domains [9,10]. Each β-sheet domain contains a TSR-I motif responsible for the interaction of PTN with heparin [9,10]. In previous studies, we have demonstrated that the C-TSR-I domain is implicated in the angiogenic effects of PTN [10,16]. Hence, these observations support the idea that NRP-1 binds to heparin-binding proteins through a heparin mimetic site. It is tempting to speculate that the recently characterized glycosaminoglycan side chains that decorate the extracellular portion of NRP-1 act as a molecular domain interacting with a heparin-binding growth factor such as PTN [37,39].

Receptor signaling is the result of a series of precisely orchestrated steps initiated at the plasma membrane after ligand binding. In this process, ligands not only bind to the extracellular domain of TKRs but, in many cases, interact with additional molecules on the cell surface acting as co-receptors [38,40]. Receptors are subsequently internalized by endocytosis and either recycled to the plasma membrane or degraded [35,41]. Biochemical analysis indicated that PTN rapidly induced NRP-1 internalization. Confocal microscopy analysis of tumor and endothelial cells demonstrated that NRP-1 predominantly localized in cytoplasm and in perinuclear regions after 15 minutes of stimulation with PTN. Interestingly, after 1 hour of stimulation with PTN, the NRP-1 was partially reexposed at the cell surface, where it presumably initiates a new round of ligand

binding and receptor activation, thereby prolonging PTN signaling to downstream targets. Ballmer-Hofer et al., showed that association of VEGFR-2 with NRP-1 promotes increased signal output by p38 MAP kinase that is only weakly activated in the absence of NRP-1[42]. Other studies indicated that NRP-1 allows addition features in signaling and act by recruiting specific pathways, such as p130^{Cas}phosphorylation[27,37]. Our results also suggest that the redistribution of NRP-1 may be associated, at least in part, with endosome recycling. Indeed, numerous studies have demonstrated that NRP-1 is required for maximum cell signaling by capturing growth factors such as VEGF $A_{165}$and sema3A, regulating their specific receptors expression, stability, endocytosis, and recycling[35,41,42]. Targeted recycling of endocytic vesicles is known to play an important role in generating cell polarity. In endothelial cell migration, the internalized growth factor receptor is recycled to the leading edge of the cell [43]. This leads to increased concentration of receptor in the forward protrusion, and it has been proposed that this sensitizes the cell to chemotaxic signaling [44,45].

A highly relevant question addressed in this study was how NRP-1 could affect PTN-induced signaling. We have shown that PTN stimulates Akt, p44/42 MAPK, and FAK tyrosine phosphorylation and that this response is almost suppressed by NRP-1 silencing. It has already been demonstrated that the mitogenic, angiogenic, and transforming activities of PTN were initially linked to the high--affinity tyrosine kinase receptor, ALK, in a process mediated by the Akt and p44/42 MAPK signaling pathways [13]. The cell migration and adhesion activities of PTN were associated to RPTPβ/ζ and mediated by Src, FAK, and p44/42 MAPK [46]. The fact that NRP-1

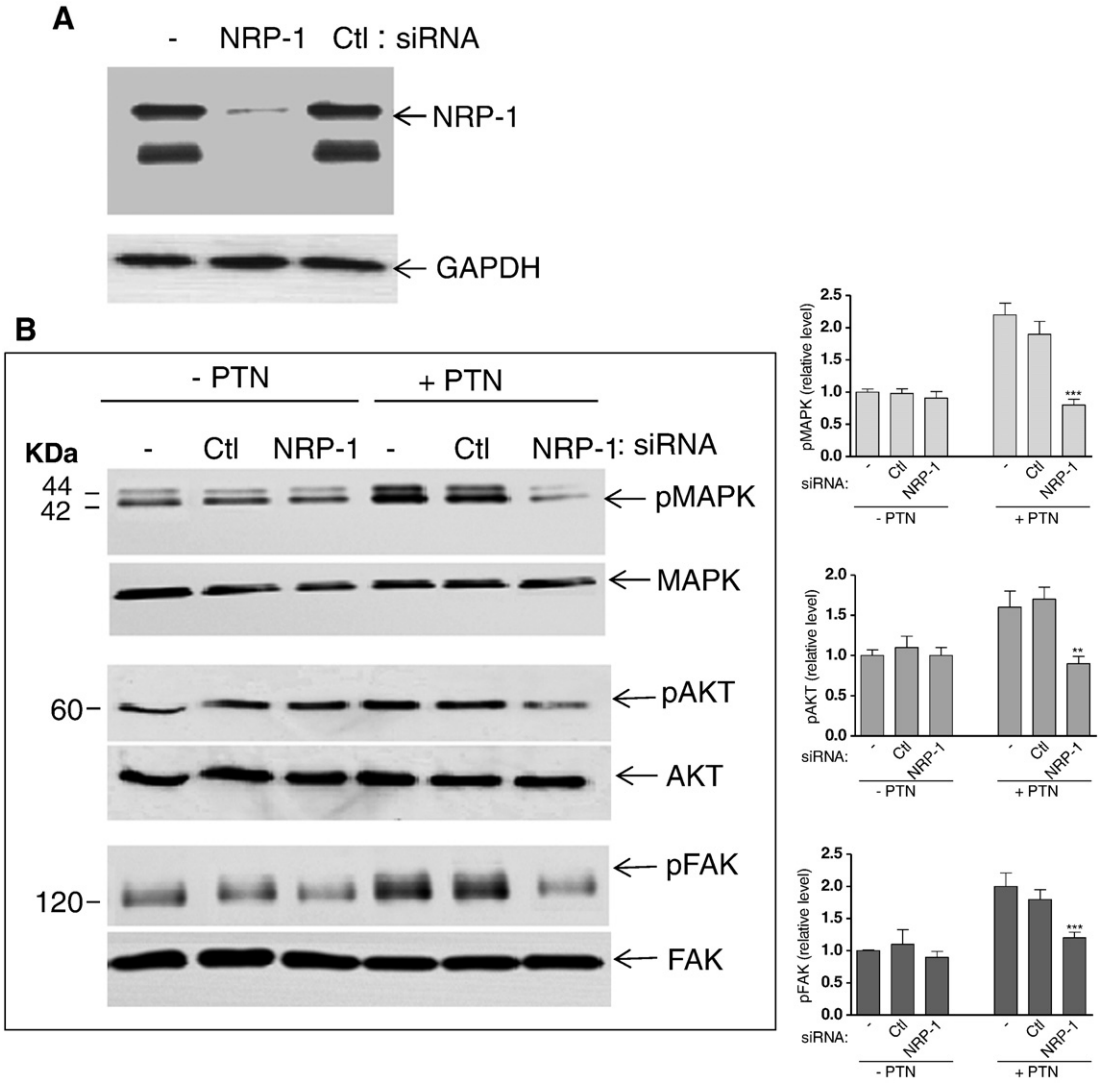

Figure 5. NRP-1 and PTN interaction activates MAPK, PI3K, and FAK pathways. (A) PC3 cells were transiently transfected with NRP-1 siRNA or with control siRNA. NRP-1 protein level was evaluated by IB. (B) NRP-1 knockdown reduced PTN-induced signaling. Transfected PC3 cells were serum starved overnight and then incubated with PTN (100 ng/ml) for 15 minutes at 37°C. Cell lysates were analyzed by IB with anti–phospho-MAPK (ERK1/2), phospho-Akt, and phospho-FAK tyr925 as well as anti-total MAPK, Akt, and FAK. Ctl: control. The phospho-protein levels obtained by scanning densitometry were normalized to total protein, respectively. Results shown are representative of three independent experiments. Bars, SEM. $^{**}P < .01$; $^{***}P < .001$ when compared with respective controls (−, Ctl). (C) Transfected PC3 cells were serum starved overnight and then incubated with VEGF A_{165} (50 ng/ml) for 15 minutes at 37°C. (D) Transfected PC3 cells were serum starved overnight and then incubated with FGF2 (50 ng/ml) for 15 minutes at 37°C. Immunoblotting was done as described above.

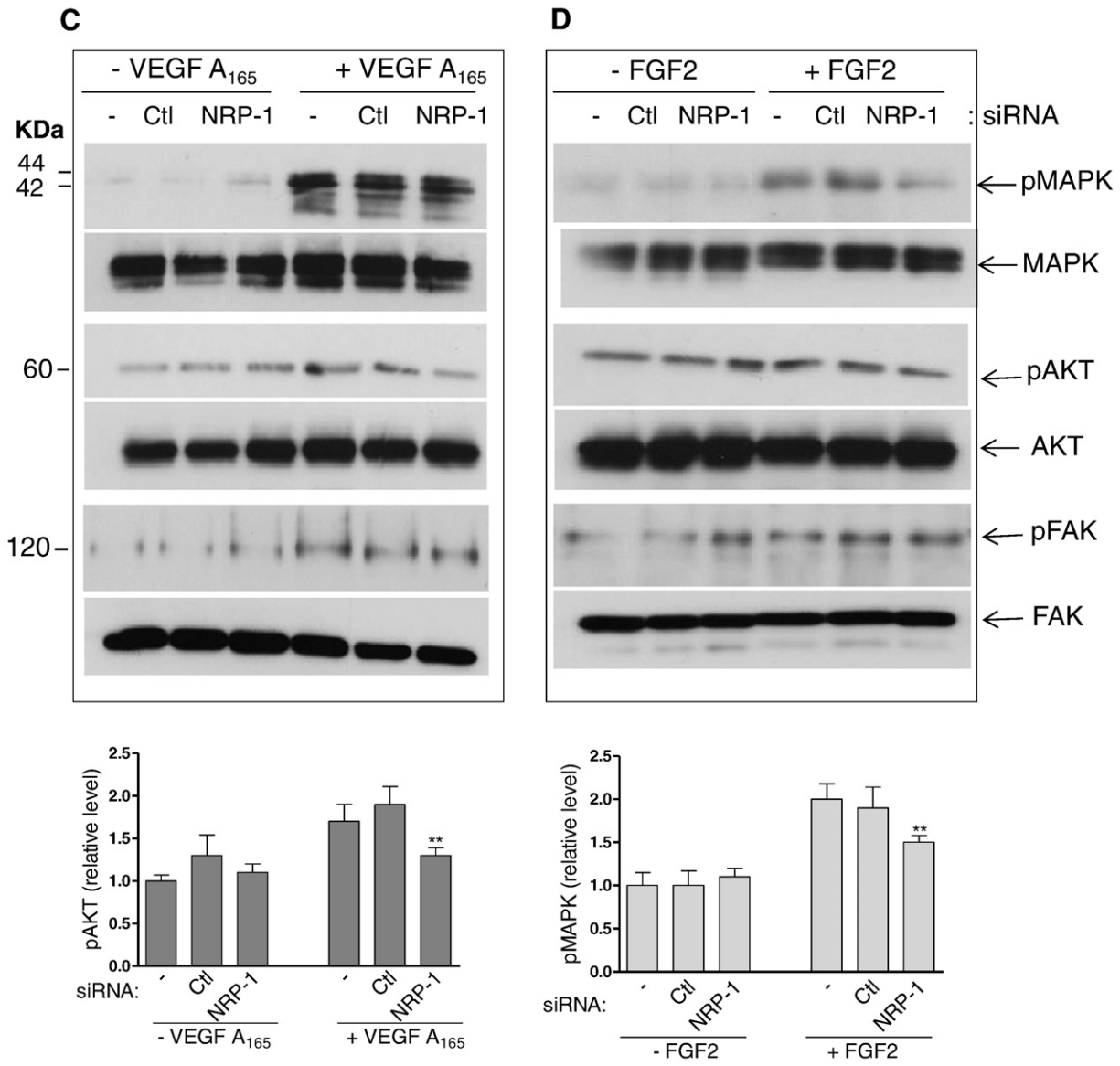

Figure 5. (*continued.*)

knockdown inhibits pathways that are stimulated by PTN via ALK and RPTPβ/ζ receptors can be explained by an interaction between NRP-1 and the other PTN receptors. Indeed, in this study, we show that, in addition to NRP-1, GST-PTN fusion protein was also able to bind ALK and RPTPβ/ζ. Thus, it appears that, in addition to ALK and RPTPβ/ζ, PTN induced cellular signaling via NRP-1 and that the molecular mechanism for cross talk and signaling involved warrants further experimental work.

Recent studies have demonstrated the importance of the p44/42 MAPK and Akt signaling pathway in cancer cell migration. The kinase Akt is activated by a wide range of stimuli, such as growth factors and cytokines, and has been implicated in cell survival, proliferation, and migration [47]. In addition, recent reports have demonstrated that the inhibitory effect of semaphorin 3B on the Akt pathway observed in numerous tumor cells was linked to NRP-1 cell expression [48]. FAK is a cytoplasmic protein tyrosine kinase that plays an important role in cell motility and survival. The signaling mediated by FAK operates via activation of the PI3K/Akt pathway, which in turn promotes cancer cell migration and invasion [49,50]. The recruitment of Src family kinases results in the phosphorylation of FAK at tyrosine residues 407, 576, 871, and 925. The conclusion that NRP-1 is important for PTN-induced endothelial cell migration and tumor cell invasion is supported by the effects of NRP-1 siRNA and NRP-1 antibodies. NRP-1 knockdown or blocking completely inhibited HUVEC migration and PTN-induced tumor cell invasion. Therefore, these results indicate that blocking NRP-1 expression at least partially inhibits cell migration and invasion in p44/42 MAPK, Akt, and FAK. This signaling pathway seems to be NRP-1/PTN interaction specific. Indeed, previous studies indicated that NRP-1 signaling through $p130^{Cas}$ tyrosine phosphorylation is essential for growth factors like VEGF A_{165}– and HGF-mediated cell migration [51].

In conclusion, we show for the first time that NRP-1 is a receptor for PTN that modulates its cell-trafficking and signaling pathways, enhanced cell migration, and invasion. In addition, our results indicated that the PTN signaling pathways induced cell motility seems to be NRP-1 / PTN interaction specific. This study suggests that NRP-1 and PTN overexpression and interaction contribute to

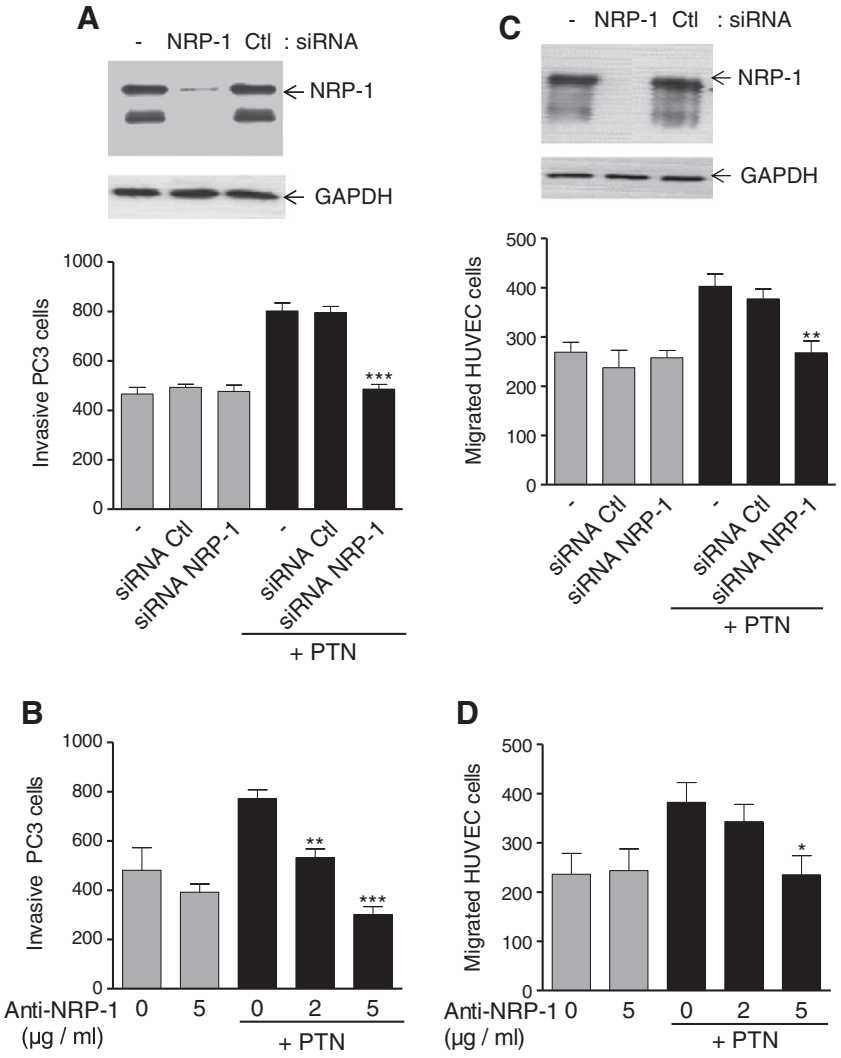

Figure 6. NRP-1 is involved in cell migration and invasion activities of PTN. (A) NRP-1 inhibition decreased PTN-induced PC3 cell invasion. siRNA-transfected PC3 cells were seeded on the top of Matrigel-coated chambers. The bottom chambers were filled with medium containing 100 ng/ml of PTN, and chemotaxis toward PTN was determined after 14 hours of incubation. (B) The bottom chambers were filled with medium containing PTN (100 ng/ml) in the presence or not of anti–NRP-1 antibody, and the chemotaxis of PC3 cells toward PTN was determined after 14 hours of incubation. (C) NRP-1 inhibition decreased HUVECs migration. HUVECs transfected with NRP-1 siRNA were plated in the top wells, either addition of PTN (100 ng/ml) in the bottom wells and chemotaxis toward PTN was determined after 6 hours of incubation. (D) HUVECs were plated on the top of wells, and the bottom chambers were filled with medium containing PTN (100 ng/ml) in the presence or not of anti–NRP-1 antibody, and the migration towards PTN was determined after 6 hours of incubation. Bars, SEM. *$P < .05$; **$P < .01$; ***$P < .001$ when compared with respective controls. Ctl: control.

cancer malignancy. Consequently, strategies aimed to inhibit NRP-1/PTN interaction may have a potential in cancer therapy.

Conflict of Interest

The authors declare no conflict of interest.

References

[1] Rauvala H (1989). An 18-kd heparin-binding protein of developing brain that is distinct from fibroblast growth factors. *EMBO J* **8**(10), 2933–2941.

[2] Wellstein A, Fang WJ, Khatri A, Lu Y, Swain SS, Dickson RB, Sasse J, Riegel AT, and Lippman ME (1992). A heparin-binding growth factor secreted from breast cancer cells homologous to a developmentally regulated cytokine. *J Biol Chem* **267**(4), 2582–2587.

[3] Bernard-Pierrot I, Delbe J, Caruelle D, Barritault D, Courty J, and Milhiet PE (2001). The lysine-rich C-terminal tail of heparin affin regulatory peptide is required for mitogenic and tumor formation activities. *J Biol Chem* **276**(15), 12228–12234.

[4] Muramatsu T (2002). Midkine and pleiotrophin: two related proteins involved in development, survival, inflammation and tumorigenesis. *J Biochem* **132**(3), 359–371.

[5] Chauhan AK, Li YS, and Deuel TF (1993). Pleiotrophin transforms NIH 3T3 cells and induces tumors in nude mice. *Proc Natl Acad Sci U S A* **90**(2), 679–682.

[6] Hamma-Kourbali Y, Bermek O, Bernard-Pierrot I, Karaky R, Martel-Renoir D, Frechault S, Courty J, and Delbe J (2011). The synthetic peptide P111-136 derived from the C-terminal domain of heparin affin regulatory peptide inhibits tumour growth of prostate cancer PC-3 cells. *BMC Cancer* **11**, 212.

[7] Bermek O, Diamantopoulou Z, Polykratis A, Dos Santos C, Hamma-Kourbali Y, Burlina F, Delbe J, Chassaing G, Fernig DG, and Katsoris P, et al (2007). A basic peptide derived from the HARP C-terminus inhibits anchorage-independent growth of DU145 prostate cancer cells. *Exp Cell Res* **313**(19), 4041–4050.

[8] Perez-Pinera P, Chang Y, and Deuel TF (2007). Pleiotrophin, a multifunctional tumor promoter through induction of tumor angiogenesis, remodeling of the tumor microenvironment, and activation of stromal fibroblasts. *Cell Cycle* **6**(23), 2877–2883.

[9] Raulo E, Tumova S, Pavlov I, Pekkanen M, Hienola A, Klankki E, Kalkkinen N, Taira T, Kilpelainen I, and Rauvala H (2005). The two thrombospondin type I

repeat domains of the heparin-binding growth-associated molecule bind to heparin/heparan sulfate and regulate neurite extension and plasticity in hippocampal neurons. *J Biol Chem* **280**(50), 41576–41583.
[10] Hamma-Kourbali Y, Bernard-Pierrot I, Heroult M, Dalle S, Caruelle D, Milhiet PE, Fernig DG, Delbe J, and Courty J (2008). Inhibition of the mitogenic, angiogenic and tumorigenic activities of pleiotrophin by a synthetic peptide corresponding to its C-thrombospondin repeat-I domain. *J Cell Physiol* **214**(1), 250–259.
[11] Raulo E, Chernousov MA, Carey DJ, Nolo R, and Rauvala H (1994). Isolation of a neuronal cell surface receptor of heparin binding growth-associated molecule (HB-GAM). Identification as N-syndecan (syndecan-3). *J Biol Chem* **269**(17), 12999–13004.
[12] Maeda N, Hamanaka H, Shintani T, Nishiwaki T, and Noda M (1994). Multiple receptor-like protein tyrosine phosphatases in the form of chondroitin sulfate proteoglycan. *FEBS Lett* **354**(1), 67–70.
[13] Stoica GE, Kuo A, Aigner A, Sunitha I, Souttou B, Malerczyk C, Caughey DJ, Wen D, Karavanov A, and Riegel AT, et al (2001). Identification of anaplastic lymphoma kinase as a receptor for the growth factor pleiotrophin. *J Biol Chem* **276**(20), 16772–16779.
[14] Said EA, Courty J, Svab J, Delbe J, Krust B, and Hovanessian AG (2005). Pleiotrophin inhibits HIV infection by binding the cell surface-expressed nucleolin. *FEBS J* **272**(18), 4646–4659.
[15] Polykratis A, Katsoris P, Courty J, and Papadimitriou E (2005). Characterization of heparin affin regulatory peptide signaling in human endothelial cells. *J Biol Chem* **280**(23), 22454–22461.
[16] Heroult M, Bernard-Pierrot I, Delbe J, Hamma-Kourbali Y, Katsoris P, Barritault D, Papadimitriou E, Plouet J, and Courty J (2004). Heparin affin regulatory peptide binds to vascular endothelial growth factor (VEGF) and inhibits VEGF-induced angiogenesis. *Oncogene* **23**(9), 1745–1753.
[17] He Z and Tessier-Lavigne M (1997). Neuropilin is a receptor for the axonal chemorepellent Semaphorin III. *Cell* **90**(4), 739–751.
[18] Soker S, Takashima S, Miao HQ, Neufeld G, and Klagsbrun M (1998). Neuropilin-1 is expressed by endothelial and tumor cells as an isoform-specific receptor for vascular endothelial growth factor. *Cell* **92**(6), 735–745.
[19] Staton CA, Kumar I, Reed MW, and Brown NJ (2007). Neuropilins in physiological and pathological angiogenesis. *J Pathol* **212**(3), 237–248.
[20] Kawasaki T, Kitsukawa T, Bekku Y, Matsuda Y, Sanbo M, Yagi T, and Fujisawa H (1999). A requirement for neuropilin-1 in embryonic vessel formation. *Development* **126**(21), 4895–4902.
[21] Fujisawa H (2004). Discovery of semaphorin receptors, neuropilin and plexin, and their functions in neural development. *J Neurobiol* **59**(1), 24–33.
[22] Bagri A, Tessier-Lavigne M, and Watts RJ (2009). Neuropilins in tumor biology. *Clin Cancer Res* **15**(6), 1860–1864.
[23] Guttmann-Raviv N, Kessler O, Shraga-Heled N, Lange T, Herzog Y, and Neufeld G (2006). The neuropilins and their role in tumorigenesis and tumor progression. *Cancer Lett* **231**(1), 1–11.
[24] Hansel DE, Wilentz RE, Yeo CJ, Schulick RD, Montgomery E, and Maitra A (2004). Expression of neuropilin-1 in high-grade dysplasia, invasive cancer, and metastases of the human gastrointestinal tract. *Am J Surg Pathol* **28**(3), 347–356.
[25] Gagnon ML, Bielenberg DR, Gechtman Z, Miao HQ, Takashima S, Soker S, and Klagsbrun M (2000). Identification of a natural soluble neuropilin-1 that binds vascular endothelial growth factor: In vivo expression and antitumor activity. *Proc Natl Acad Sci U S A* **97**(6), 2573–2578.
[26] Jia H, Cheng L, Tickner M, Bagherzadeh A, Selwood D, and Zachary I (2010). Neuropilin-1 antagonism in human carcinoma cells inhibits migration and enhances chemosensitivity. *Br J Cancer* **102**(3), 541–552.
[27] Zachary IC (2011). How neuropilin-1 regulates receptor tyrosine kinase signalling: the knowns and known unknowns. *Biochem Soc Trans* **39**(6), 1583–1591.
[28] Rasband WS (1997-2012). ImageJ. National Institutes of Health; 1997-2012 .
[29] Griffa A, Garin N, and Sage D (2010). Comparison of Deconvolution Software in 3D Microscopy. A User Point of View. *Imaging Microsc* **1**, 43–45.
[30] Vonesch C and Unser M (2008). A Fast Thresholded Landweber Algorithm for Wavelet-Regularized Multidimensional Deconvolution. *IEEE Trans Image Process* **17**, 539–549.
[31] Otsu N (1979). A threshold selection method from gray-level histograms. *IEEE Trans Syst Man Cybern* , 62–66.
[32] Baba T, Kariya M, Higuchi T, Mandai M, Matsumura N, Kondoh E, Miyanishi M, Fukuhara K, Takakura K, and Fujii S (2007). Neuropilin-1 promotes unlimited growth of ovarian cancer by evading contact inhibition. *Gynecol Oncol* **105**(3), 703–711.
[33] Perez-Pinera P, Zhang W, Chang Y, Vega JA, and Deuel TF (2007). Anaplastic lymphoma kinase is activated through the pleiotrophin/receptor protein-tyrosine phosphatase beta/zeta signaling pathway: an alternative mechanism of receptor tyrosine kinase activation. *J Biol Chem* **282**(39), 28683–28690.
[34] Vacherot F, Delbe J, Heroult M, Barritault D, Fernig DG, and Courty J (1999). Glycosaminoglycans differentially bind HARP and modulate its biological activity. *J Biol Chem* **274**(12), 7741–7747.
[35] Narazaki M and Tosato G (2006). Ligand-induced internalization selects use of common receptor neuropilin-1 by VEGF165 and semaphorin3A. *Blood* **107**(10), 3892–3901.
[36] Mikelis C, Koutsioumpa M, and Papadimitriou E (2007). Pleiotrophin as a possible new target for angiogenesis-related diseases and cancer. *Recent Pat Anticancer Drug Discov* **2**(2), 175–186.
[37] Frankel P, Pellet-Many C, Lehtolainen P, D'Abaco GM, Tickner ML, Cheng L, and Zachary IC (2008). Chondroitin sulphate-modified neuropilin 1 is expressed in human tumour cells and modulates 3D invasion in the U87MG human glioblastoma cell line through a p130Cas-mediated pathway. *EMBO Rep* **9**(10), 983–989.
[38] Hamerlik P, Lathia JD, Rasmussen R, Wu Q, Bartkova J, Lee M, Moudry P, Bartek Jr J, Fischer W, and Lukas J, et al (2012). Autocrine VEGF-VEGFR2--Neuropilin-1 signaling promotes glioma stem-like cell viability and tumor growth. *J Exp Med* **209**(3), 507–520.
[39] Shintani Y, Takashima S, Asano Y, Kato H, Liao Y, Yamazaki S, Tsukamoto O, Seguchi O, Yamamoto H, and Fukushima T, et al (2006). Glycosaminoglycan modification of neuropilin-1 modulates VEGFR2 signaling. *EMBO J* **25**(13), 3045–3055.
[40] Ball SG, Bayley GC, Shuttleworth CA, and Kielty CM (2010). Neuropilin-1 regulates platelet-derived growth factor receptor signalling in mesenchymal stem cells. *Biochem J* **427**(1), 29–40.
[41] De Wit J, De Winter F, Klooster J, and Verhaagen J (2005). Semaphorin 3A displays a punctate distribution on the surface of neuronal cells and interacts with proteoglycans in the extracellular matrix. *Mol Cell Neurosci* **29**(1), 40–55.
[42] Ballmer-Hofer K, Andersson AE, Ratcliffe LE, and Berger P (2011). Neuropilin-1 promotes VEGFR-2 trafficking through Rab11 vesicles thereby specifying signal output. *Blood* **118**(3), 816–826.
[43] Gampel A, Moss L, Jones MC, Brunton V, Norman JC, and Mellor H (2006). VEGF regulates the mobilization of VEGFR2/KDR from an intracellular endothelial storage compartment. *Blood* **108**(8), 2624–2631.
[44] Gerhardt H, Golding M, Fruttiger M, Ruhrberg C, Lundkvist A, Abramsson A, Jeltsch M, Mitchell C, Alitalo K, and Shima D, et al (2003). VEGF guides angiogenic sprouting utilizing endothelial tip cell filopodia. *J Cell Biol* **161**(6), 1163–1177.
[45] Valdembri D, Caswell PT, Anderson KI, Schwarz JP, Konig I, Astanina E, Caccavari F, Norman JC, Humphries MJ, and Bussolino F, et al (2009). Neuropilin-1/GIPC1 signaling regulates alpha5beta1 integrin traffic and function in endothelial cells. *PLoS Biol* **7**(1), 0115–0132.
[46] Diamantopoulou Z, Bermek O, Polykratis A, Hamma-Kourbali Y, Delbe J, Courty J, and Katsoris P (2010). A Pleiotrophin C-terminus peptide induces anti-cancer effects through RPTPbeta/zeta. *Mol Cancer* **9**, 224.
[47] Manning BD and Cantley LC (2007). AKT/PKB signaling: navigating downstream. *Cell* **129**(7), 1261–1274.
[48] Castro-Rivera E, Ran S, Brekken RA, and Minna JD (2008). Semaphorin 3B inhibits the phosphatidylinositol 3-kinase/Akt pathway through neuropilin-1 in lung and breast cancer cells. *Cancer Res* **68**(20), 8295–8303.
[49] Benelli R, Vene R, Ciarlo M, Carlone S, Barbieri O, and Ferrari N (2012). The AKT/NF-kappaB inhibitor xanthohumol is a potent anti-lymphocytic leukemia drug overcoming chemoresistance and cell infiltration. *Biochem Pharmacol* **83**(12), 1634–1642.
[50] Shukla S, Maclennan GT, Hartman DJ, Fu P, Resnick MI, and Gupta S (2007). Activation of PI3K-Akt signaling pathway promotes prostate cancer cell invasion. *Int J Cancer* **121**(7), 1424–1432.
[51] Evans IM, Yamaji M, Britton G, Pellet-Many C, Lockie C, Zachary IC, and Frankel P (2011). Neuropilin-1 signaling through p130Cas tyrosine phosphorylation is essential for growth factor-dependent migration of glioma and endothelial cells. *Mol Cell Biol* **31**(6), 1174–1185.